

M. D'Abramo<sup>1</sup>  
A. C. Rinaldi<sup>2</sup>  
A. Bozzi<sup>3</sup>  
A. Amadei<sup>4</sup>  
G. Mignogna<sup>5</sup>  
A. Di Nola<sup>1</sup>  
M. Aschi<sup>6</sup>

<sup>1</sup> Dipartimento di Chimica,  
Università di Roma "La  
Sapienza," Roma, Italia

<sup>2</sup> Dipartimento di Scienze e  
Tecnologie Biomediche,  
Sezione di Chimica Biologica e  
Biotecnologie Biochimiche,  
Università di Cagliari,  
Monserrato, Italia

<sup>3</sup> Dipartimento di Scienze e  
Tecnologie Biomediche,  
Università de L'Aquila,  
L'Aquila, Italia

# Conformational Behavior of Temporin A and Temporin L in Aqueous Solution: A Computational/Experimental Study

<sup>4</sup> Dipartimento di Scienze e Tecnologie  
Chimiche, Università di Roma,  
"Tor Vergata," Roma, Italia

<sup>5</sup> Dipartimento di Scienze Biochimiche "A.  
Rossi Fanelli" and CNR, Università "La  
Sapienza," Roma, Italia

<sup>6</sup> Dipartimento di Chimica, Ingegneria  
Chimica e Materiali, Università de L'Aquila,  
L'Aquila, Italia

Received 11 July 2005;  
revised 20 October 2005;  
accepted 21 October 2005

Published online 31 October 2005 in Wiley InterScience  
(www.interscience.wiley.com). DOI 10.1002/bip.20404

**Abstract:** Molecular dynamics (MD) simulations and circular dichroism (CD) experiments were carried out on aqueous temporin A and L, two short peptides belonging to an interesting class of natural substances known to be active mainly against Gram-positive/negative bacteria and fungi. Experimental results indicate the higher propensity of temporin L, with respect to temporin A, in forming  $\alpha$ -helical structures. These results were revisited by long-timescale MD simulations, in which their  $\alpha$ -helical propensity was investigated in the absence of trifluoroethanol. Results clearly show the higher stability of  $\alpha$ -helix conformations in temporin L; moreover, an interestingly strong mechanical analogy emerges since both temporins show the same residue interval (from 7 to 10) as the most energetically accessible for  $\alpha$ -helix formation. Such studies provide some intriguing structural and mechanical evidence that may help in better understanding and rationalizing the conformational behaviour of temporins in water solution and, ultimately, the inner principles of their microbial targets selectivity and mechanism of action at the level of cell membranes. © 2005 Wiley Periodicals, Inc. *Biopolymers* 81: 215–224, 2006

This article was originally published online as an accepted preprint. The "Published Online" date corresponds to the preprint version. You can request a copy of the preprint by emailing the *Biopolymers* editorial office at [biopolymers@wiley.com](mailto:biopolymers@wiley.com)

**Keywords:** temporins; antimicrobial peptides; molecular dynamics; free energy landscape; circular dichroism

Correspondence to: M. Aschi; e-mail: [aschi@caspur.it](mailto:aschi@caspur.it)  
Contract grant sponsor: Italian Ministry of Education, University  
and Research.

*Biopolymers*, Vol. 81, 215–224 (2006)  
© 2005 Wiley Periodicals, Inc.



## INTRODUCTION

Gene-encoded antimicrobial peptides are key effectors of the so-called innate immunity. An ever increasing number of these molecules are being isolated from a vast array of biological sources, either prokaryotic and eukaryotic, including humans, which they protect from the invasion of bacteria, protozoa, fungi, and viruses.<sup>1,2</sup> Antimicrobial peptides display an extreme diversity in their primary and secondary structures, and usually have a rather large spectrum of antibiotic activity. The low selectivity and the fast killing of microbes are key features of the peptide-based defenses that characterize its function as an “instant” immune system against microbial invaders, as recently highlighted by Hans Boman.<sup>3</sup> This immediate host response to infections plays an important role not only in invertebrates, which exclusively depend on it, but also in higher vertebrates, where it comes into action before the adaptive immunity is activated.<sup>4,5</sup> To face the challenge posed by the spreading resistance of pathogenic microbial strains to conventional antibiotics, the production of substitute antibiotics with new activities and resistance-avoiding properties has become an emergency. Among the possible candidates, antimicrobial peptides came recently under the spotlight as attractive molecules to be potentially developed as therapeutic anti-infective agents<sup>1,6</sup> and even as food preservatives.<sup>7</sup> This spurred the initiation of studies aimed at understanding their mode(s) of action.

A large body of evidence proves that killing of microbes by antimicrobial peptides involves their initial interaction with the cytoplasmic membrane.<sup>8,9</sup> The details of this interaction, and how this actually leads to microbial death, however, are largely unknown. Amphibians have proved to be an incredibly rich source of antimicrobial peptides, stored in skin granules destined for extracellular secretion.<sup>10,11</sup> Temporins are a family of related antimicrobial peptides first isolated from the skin of the European red frog *Rana temporaria*.<sup>12</sup> Many other members of this group, counting now over 40 peptides, have later been found in several *Rana* species and also in the venom of wasps.<sup>13–15</sup> Structurally, temporins are characterized by being short (10–14 residues), by bearing a net positive charge at neutral pH value, and by their potential to adopt an amphipathic  $\alpha$ -helix structure upon contact with membranes or when in hydrophobic environments. The derived consensus sequence for 36 frog-derived temporins is FLP-LIASLLSKLL-NH<sub>2</sub>. Previously, temporins were found to be active against Gram-positive/negative bacteria and fungi, and to bind and permeate both artificial and

biological membranes.<sup>10,11,16–18</sup> Besides providing information on the behavior of temporins, a wider understanding of their modes of interaction with lipid membranes and, more generally, of their antibacterial mechanism, may well prove to be paradigmatic for other short, naturally occurring peptides.

Many antimicrobial peptides, belonging to different structural classes, present an unstructured conformation in aqueous solution, and a marked increase in secondary structure content with the assumption of an amphipathic design usually takes place when these molecules are transferred into a membrane-like environment.<sup>19,20</sup> In this respect, however, a deep knowledge of the structural–conformational features driving this drastic rearrangement to elicit the peptides' antimicrobial potential is currently lacking. Computational methods may provide one of the most efficient and reliable tools available nowadays to tackle this important issue.<sup>21,22</sup> As a contribution, we therefore decided to carry out molecular dynamics (MD) simulations specifically addressing the behavior in water solution of two antimicrobial peptides belonging to the temporin family, namely temporin A (FLPL-IGRVLSGIL) and temporin L (FVQWFSKFLGRIL). Our approach is based on a joint application of experimental (circular dichroism, CD) measurements and long-timescale MD simulations, with the precise aim of evaluating the free energy conformational landscape of both peptides and their folding propensity in water solution (i.e., in the absence of typical helical-structure stabilizers such as trifluoroethanol, TFE), looking for built-in conformational characteristics that could plausibly rationalize the different spectrum and level of activity on membrane-enveloped targets recorded for temporins A and L. In particular, temporin A is preferentially active against Gram-positive bacterial strains,<sup>13,16</sup> including some clinically important antibiotic-resistant ones,<sup>13</sup> displays a moderately lytic against human erythrocyte<sup>16</sup> and, as recently shown, kills efficiently the human parasitic protozoan *Leishmania*.<sup>23</sup> On the other side, temporin L has the highest activity among all temporins studied to date against human erythrocytes, fungi, and bacteria, including Gram-negative strains.<sup>10,24</sup>

## EXPERIMENTAL AND COMPUTATIONAL METHODS

### CD Measurements

CD measurements were carried out with a Jasco J710 spectropolarimeter, equipped with a DP 520 processor, at 25°C, using a quartz cell of 2-mm path length. The peptide samples (65  $\mu$ M temporin L, 100  $\mu$ M temporin A) were pre-

pared in H<sub>2</sub>O–TFE solutions (0–80 % TFE, by volume). For each sample, five spectra were recorded at the scan rate of 20 nm/min and averaged.

## MD Simulations

We performed two MD simulations of 290-ns time length in the isochoric-isothermal (NVT) ensemble for the temporins A and L. Both the peptides were put initially in the  $\alpha$ -helix conformation, at the centre of a box filled with the single point charge (SPC) water model<sup>25</sup> at the typical water density (55.32 mol/L). The first nanosecond was considered as equilibration and then all the analysis included 289 ns. A 2-fs time step was used, the rototranslational motion was removed,<sup>26</sup> the temperature was kept fixed at 300 K by the isokinetic temperature coupling,<sup>27</sup> and the long-range electrostatics was treated by means of the Particle Mesh Ewald (PME) method.<sup>28</sup> A modified version of the Gromacs software package<sup>29</sup> and the Gromos96 force field were used. Note that during the simulations many unfolding/refolding transitions occurred, possibly indicating that the initial conformation should not, or only poorly, influence the conformational sampling of the system.

## Conformational Analysis

The main difficulty arising when a conformational analysis of a relatively large molecule is carried out is the proper definition of a “conformational coordinate,” i.e., a set of generalized coordinates providing the directions in the phase space connecting the relevant conformational states. In this respect, a powerful and rigorous approach is based on the essential dynamics (ED) analysis. Although ED is widely described in detail elsewhere,<sup>30</sup> we report some of its basic features. Briefly, by diagonalizing either C- $\alpha$  or all-atoms positional fluctuations covariance matrix, as provided by the MD simulation, we obtain a set of eigenvectors and eigenvalues. The eigenvectors represent the directions in configurational space and the eigenvalues indicate the mean square fluctuations along these axes. Sorting the eigenvectors by the size of the corresponding eigenvalues, the configurational space can be divided in a low dimensional (essential) subspace in which most of the positional fluctuations are confined, and a high dimensional subspace in which small and conformationally irrelevant vibrations occur. The projection of the trajectory onto the essential space may provide conformational free energy (see next subsection) and, virtually, all the thermodynamics of the peptide.

## Thermodynamic Analysis

The free energy change for any transition from a reference state “ref” to a generic state “i,” at constant volume and temperature, can be calculated from the probabilities  $p$  (obtained by the MD simulation) of finding the system in both states “i” and “ref”

$$\Delta A_{\text{ref},i} = -RT \ln \frac{p_i}{p_{\text{ref}}} \quad (1)$$

where  $R$  is the ideal gas constant and  $T$  the (absolute) temperature.

Moreover, combining the internal energy change  $U_{\text{ref},i} = U_i - U_{\text{ref}}$  (obtained averaging over the MD frames associated to the “i” and “ref” states) we may also evaluate the corresponding entropy variation via

$$\Delta S_{\text{ref},i} = \frac{\Delta U_{\text{ref},i} - \Delta A_{\text{ref},i}}{T} \quad (2)$$

In this article, the above equations have been used for evaluating the thermodynamics in the conformational space (hereafter called essential plane) defined by the first two essential eigenvectors obtained by the ED analysis. In this case the reference (“ref”) condition was taken, for each peptide, as the one corresponding to the absolute free-energy minimum, i.e., it was evaluated a posteriori on the basis of the resulting free energy landscape.

The same equations also provided the overall folding thermodynamics, as obtained by MD simulation data. Thus, we deliberately evaluated the global thermodynamic changes due to the transitions from completely unfolded (reference state) condition to each of the conformational states defined by an increasing number  $n$  of residues in  $\alpha$ -helix conformation (the minimum value of  $n$  was therefore set at 4). Note that the choice of the reference state does not obviously alter the thermodynamic picture. It is also important to further stress that we are following the free energy change for arranging at least four residues in the  $\alpha$ -helix conformation. Therefore, for *unfolded condition* we indicate the ensemble of structures in which such a condition is not fulfilled. On the basis of the MD results (vide infra), we found that the first two eigenvalues of the all-atoms covariance matrix could account for the largest portion of the phase space. For this reason, all the above analyses were carried out on a bidimensional essential space hereafter called “essential plane.”

## RESULTS AND DISCUSSION

### Circular Dichroism

CD spectroscopy was used to determine the conformation of synthetic temporin L and temporin A in solution by recording the spectra in water and after addition of TFE. Temporin A spectra were comparable to those obtained for the same peptide by Wade and colleagues under similar conditions, and published elsewhere.<sup>13</sup> The experiments demonstrate that for both peptides an increase in TFE concentration caused a progressive change from a random coil to an  $\alpha$ -helical structure (Figure 1). In the case of temporin L, the effect was almost complete at about 20% TFE

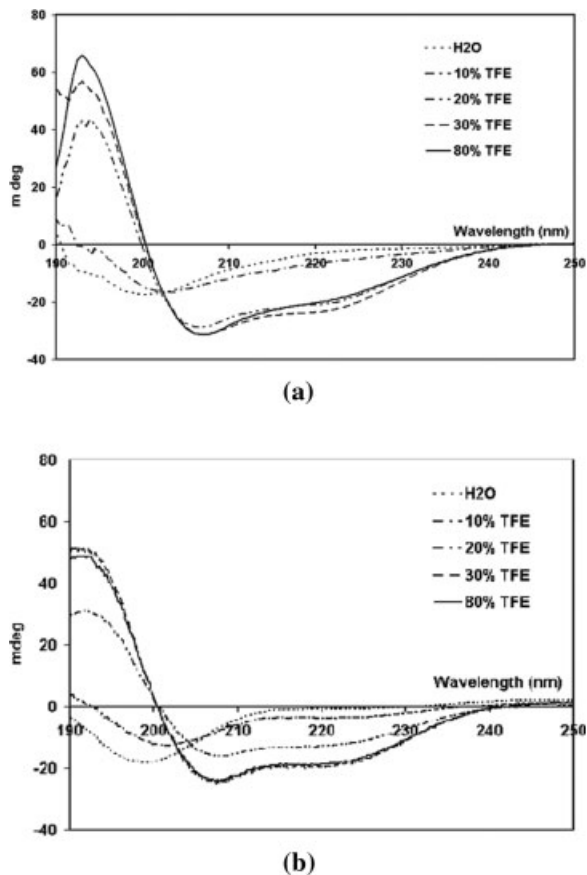


**FIGURE 1** CD spectra of temporin L (a) and temporin A (b) in water and TFE.

(Figure 1a). This is somehow at variance from what was seen with temporin A, which, although it displayed similar spectra with a minimum close to 200 nm, exhibited the maximal effect at 30% TFE (Figure 1b). Thus, in temporin L the gradual change from random coil to an  $\alpha$ -helical conformation was significantly enhanced, and the peptide became almost completely structured at a lower TFE/H<sub>2</sub>O ratio. This higher propensity to adopt an ordered conformation even in a relatively poor hydrophobic solvent, which clearly represents an intriguing difference between the two temporins, prompted us to investigate the thermodynamics as well as the energetics associated to the dynamics of the peptides in solution. In particular, MD simulations have been used in order to evaluate the “intrinsic” ability of the two temporins in forming  $\alpha$ -helices—thus their folding propensity even in the lack of TFE.

### Structural Motions

In this section we show the results of the ED analysis on the trajectories of temporins A and L, with the pre-

cise aim of identifying the main peptide internal motions in water solution. The diagonalization of the covariance matrix provides a set of eigenvectors and eigenvalues, corresponding to generalized conformational coordinates and fluctuations. Among them, only a small fraction is typically associated with significant internal motions of the system, i.e., the corresponding eigenvalues are significantly different from zero. The all-atom eigenvalues spectrum of temporin L (Figure 2) clearly shows that the first ten eigenvectors are responsible for large part of the internal motions (the same is observed for C- $\alpha$ ). Similar results were obtained for temporin A (data not shown). The link between each eigenvector and the relevant atomic structural motions can be studied by analyzing the corresponding atomic components. The results are reported in Figures 3 and 4.

In Figure 3a, the atom composition of the first two (all-atoms) eigenvectors of temporin L shows that these eigenvectors provide concerted motions mainly involving the terminal residues (Phe1, Leu13) as well as Gln3 and Lys7. Interestingly, the same analysis conducted for the first two C- $\alpha$  eigenvectors (see Figure 3b) shows that Gln3 and Lys7 are associated to almost zero components, whereas the terminal residues still correspond to high peaks. These results indicate that the structural fluctuations involving Gln3 and Lys7 in temporin L are mainly due to side-chain motions. In the case of temporin A (Figure 4a), the first two all-atoms eigenvectors largely involve terminal motions (i.e., high values of the corresponding components), but also with a significant component associated with the Arg7 side chain (see Figure 4b). At variance with temporin L, the first two C- $\alpha$  eigenvectors show the presence of four clearly separated blocks, namely the terminal residues Leu4, Ile5–Val8, and Leu9–Ser10 (see Figure 4b).

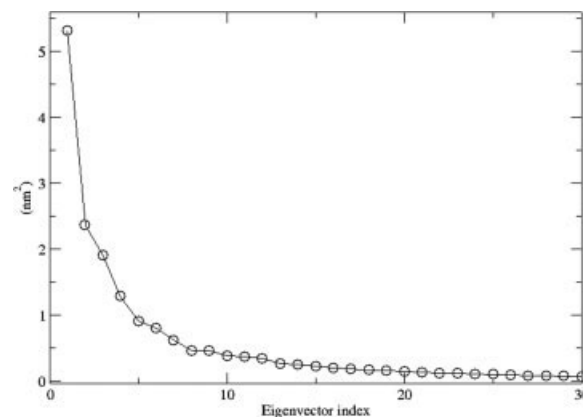


**FIGURE 2** Eigenvalues of the all-atom covariance matrix from MD simulations of temporin L.

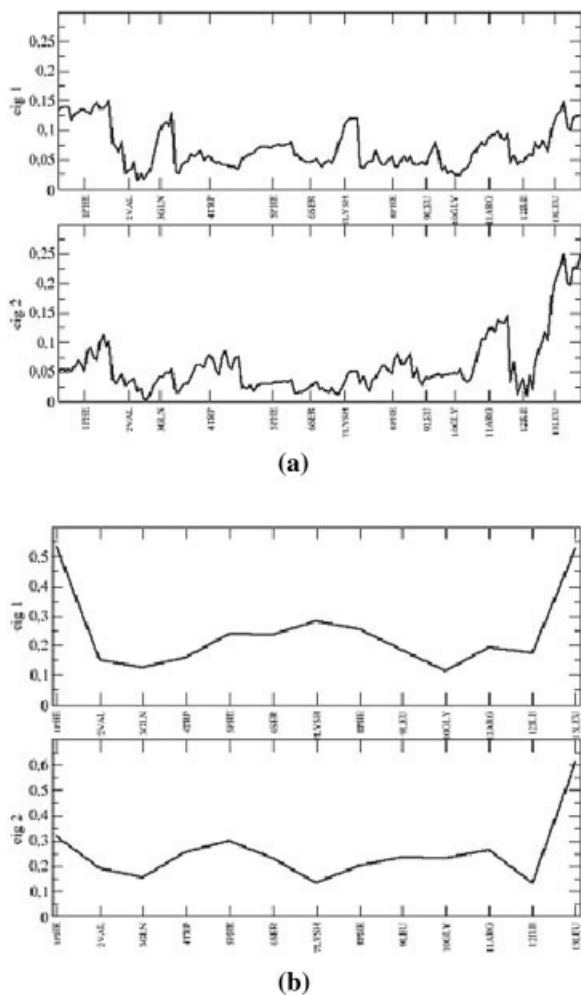


**FIGURE 3** (a) Absolute component values of the first two all-atoms eigenvectors of temporin. (b) Absolute component values of the first two C- $\alpha$  eigenvectors of temporin L.

On the basis of these preliminary results, some “dynamical” differences between the two temporins are clearly evident. Therefore, a more detailed thermodynamic inspection on the essential plane—as described in the methodological section—was carried out.

## Thermodynamics

The 300 K Helmholtz free energy surface of temporin A, as a function of the position in the essential plane, shows the absolute minimum [which provides the “ref” conformation in Eq. (1)] in the centre of the plane, and two local minima just 3–4 kJ/mol higher (Figure 5). In Figure 6 we report the corresponding 300 K entropy surface as provided by Eq. (2). It is interesting to observe that the two local free energy minima are associated with entropy values significantly lower than the absolute free energy minimum

one. At the same time, a large part of the accessible plane, corresponding to a relatively high free energy, is associated to higher entropy values. This finding clearly indicates that temporin A free energy minima are mainly determined by the internal energy (a physical condition apparently normal but not always predominant in biological molecules in solution; see Ref. 31), and that the structures characterized by higher entropy are not thermodynamically stable.

Differently from temporin A, temporin L shows a behavior characterized by a “corrugated” free energy surface with several minima (Figure 7). However, similarly to temporin A, all these free energy minima are associated to low entropy regions (Figure 8).

We show therefore that both temporins undergo a rather typical internal energy-driven conformational sampling in which high-entropy (highly disordered) structures do not represent accessible states in these conditions. In other words, temporins A and L both

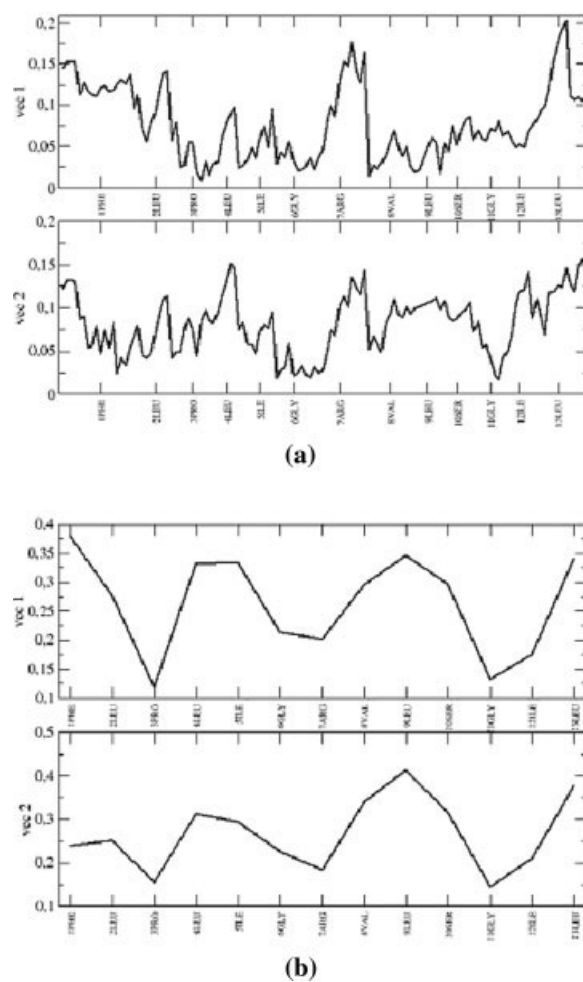


**FIGURE 4** (a) Absolute component values of the first two all-atoms eigenvectors of temporin. (b) Absolute component values of the first two C- $\alpha$  eigenvectors of temporin A.

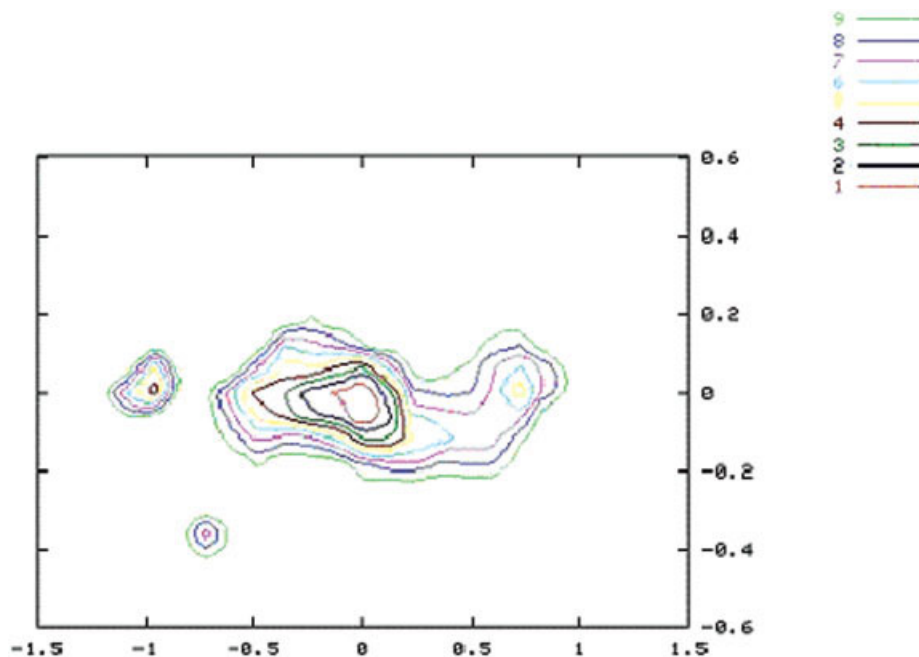


**FIGURE 5** Temporin A: 300 K Helmholtz free energy (kJ/mol) map on the all-atoms essential plane (nm).

preferentially exist in partially organized (not fully ‘unfolded’) structures characterized by low internal energy values but also relatively low entropy values. This finding clearly required a more accurate inspection; we therefore calculated the global  $\alpha$ -helix formation free energy for an increasing number of residues (from 4 to 13). The result is reported in Figure 9.

It is important to underline that a conformational state is typically considered as “folded” when at least six residues are organized in a helix structure. In Figure 9 it is evident that both temporins show in water solution a positive  $\alpha$ -helix formation free energy (i.e., essentially a thermodynamic instability) when six or more residues are involved. At the same time, it is

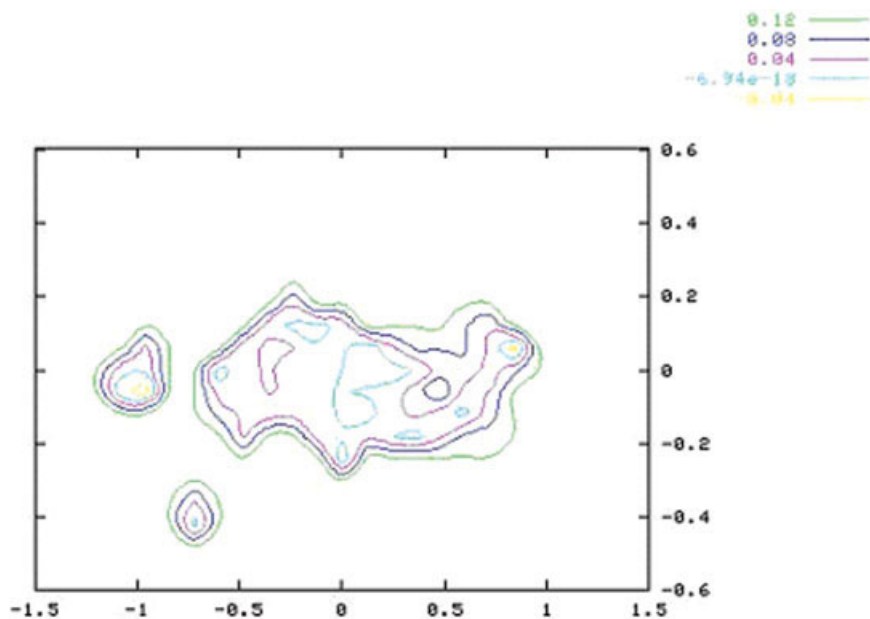


**FIGURE 6** Temporin A: 300 K entropy (J/mol K) map on the all-atoms essential plane (nm).

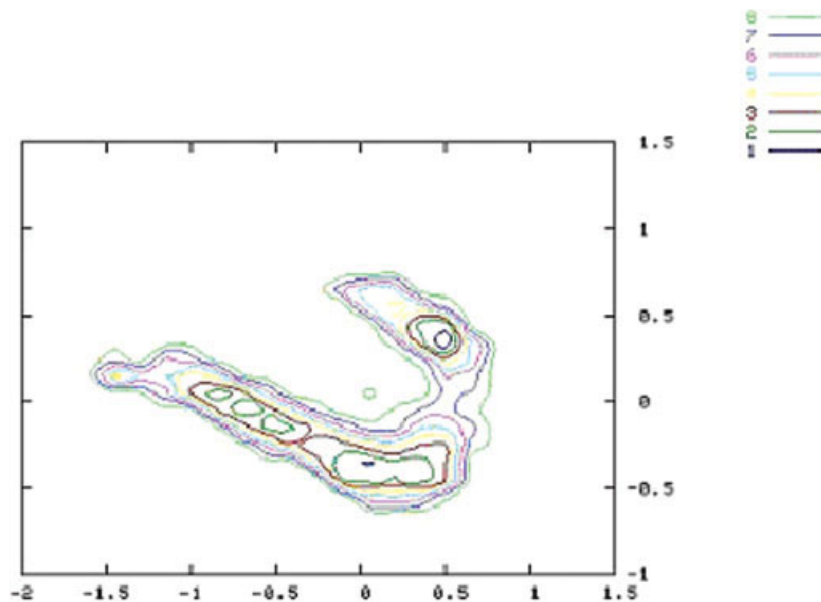


**FIGURE 7** Temporin L: 300 K Helmholtz free energy (kJ/mol) map on the all-atoms essential plane.

also evident from the same figure that temporin L is in all cases characterized by an  $\alpha$ -helix formation free energy systematically lower than temporin A, irrespective of the number of residues involved. Furthermore, when 4 or 5 residues are considered, temporin L also shows a slightly negative helix formation free energy. This finding may provide some additional information on the actual conformational state of the peptides. In particular, temporin L seems to exist basically in a “semifolded” (low-entropy) state characterized by a 4(5)-residue helix, which nicely con-

firms and strengthens the results shown in Figures 7 and 8. Moreover, the temporin L “dynamical” fingerprint reported in Figure 3b, characterized by a high fluctuation almost exclusively confined within the terminal, conceivably less “organized” (*vide infra*) residues, can also be explained at the light of these results.

In conclusion, both peptides (in water at 300 K) do not show any  $\alpha$ -helix conformation, even though temporin L, consistent with the experimental evidence obtained by CD spectroscopy (section 3.1),

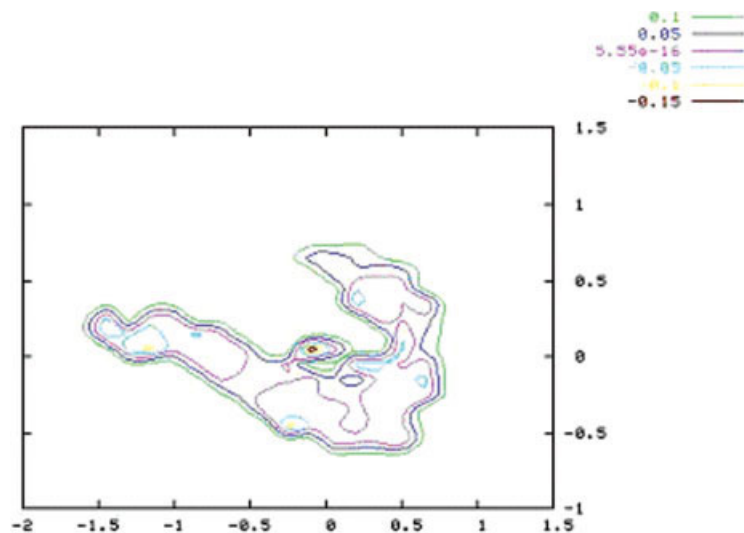


**FIGURE 8** Temporin L: 300 K entropy (J/mol K) map on the all-atoms essential plane.

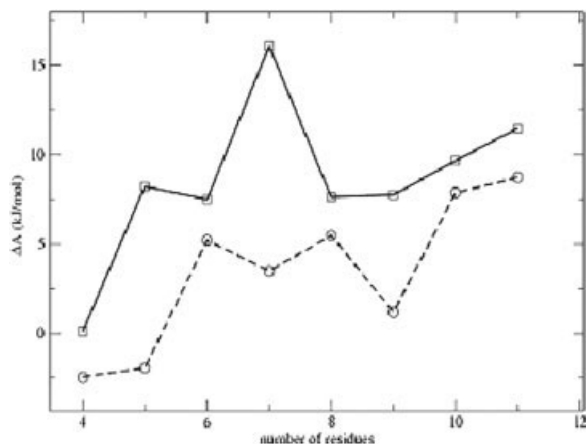


**FIGURE 9** The 300 K Helmholtz free energy of folding of temporin A (solid line) and temporin L (dashed line) as a function of the number of folded residues.

shows a higher propensity to form stable  $\alpha$ -helices in water compared to temporin A.

We also evaluated which residues specifically contribute to the  $\alpha$ -helix formation. The interesting aspect emerging from this analysis is that both peptides are characterized by a topologically identical region of  $\alpha$ -helix aggregation, as shown in Figure 10. More specifically, the first structural organization, that is the less work-intensive combination of 4 resi-

dues, involves the same positions along the sequence even in the presence of different residues. This result may provide, as far as we know for the first time, an intriguing insight into the folding mechanism, characterized by the presence of a core group of residues triggering the folding (i.e., the residues from 7 to 10) and whose thermodynamic accessibility drives the global folding propensity and, possibly, the related antimicrobial activity.

Indeed, it is conceivable that the greater antimicrobial and hemolytic activity exhibited by temporin L could be ascribed to its higher propensity to assume a folded conformation. In other words, the presence of a partially folded structure in water solution may plausibly facilitate, both thermodynamically and kinetically, the peptide folding in the microbial membrane. In addition, the higher positive charge (+3) possessed by temporin L could enhance its initial binding to the negatively charged outer plasma membrane of bacterial targets. Although both temporins are too short to span the membrane bilayer and thus form a simple transmembrane pore composed of an helical cluster (the classic “barrel-stave” model), a wealth of data indicates that temporins can insert into and damage the cellular membrane as part of their killing mechanism.<sup>10,11,16–18</sup> A number of other models (e.g., the “carpet” and “sinking-raft” models) have been proposed to account for peptide-induced

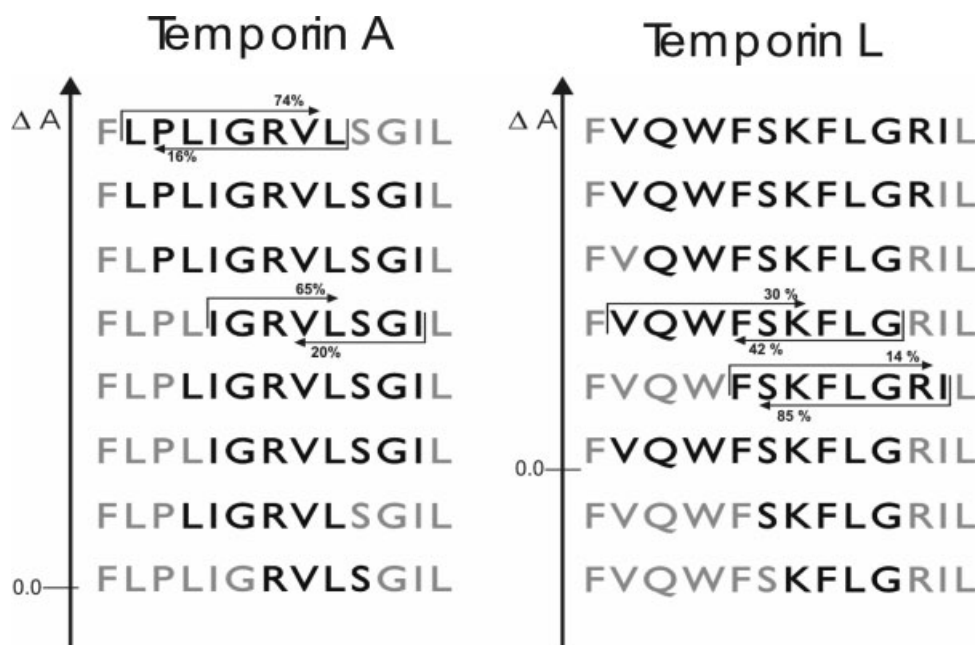


**FIGURE 10** The  $\alpha$ -helix forming residues (only the residues found to be present for more than 90% of the trajectory) are reported in bold, with the exception of the ones whose fraction is explicitly indicated) as emerged from MD simulations of temporin A (left) and L (right). The sequences are reported according to the corresponding free energy of folding (see Figure 9).

membrane permeabilization/disruption, and envisage at first the absorption of the peptide to the membrane with the helices parallel to the surface, and a subsequent mechanism of membrane destabilization that could in principle adapt also to temporins and other short linear peptides.<sup>32,33</sup> Whereas it is not yet possible to indicate precisely the molecular mechanism of interaction of temporins with lipid membranes, the present investigation suggests that the “inherent” structural features, which ultimately depend on the specific sequences, might be an essential determinant of the biological activities of these antimicrobial peptides.

## CONCLUSIONS

CD spectroscopy was used to determine the conformation of synthetic temporin L and temporin A in solution. Analysis of the resulting patterns indicates that temporin L displays a higher propensity to acquire the  $\alpha$ -helix conformation. Long-timescale MD simulations carried out on both temporins in aqueous solutions confirm the experimental observations, clearly showing that, in the case of temporin L,  $\alpha$ -helix formation free energy is always lower than that of temporin A. A more careful thermodynamic analysis indicates that both peptides exist, in aqueous solution, in a not completely random coil conformation, even if a positive Helmholtz free energy is found for the structural rearrangement into an  $\alpha$ -helix containing at least six residues. The greater  $\alpha$ -helix propensity, together with the higher net positive charge, exhibited by temporin L may provide some quantitative key aspects for proposing models of action plausibly explaining its efficacy against selected microbial targets.

AB wishes to acknowledge the financial support received from the Italian Ministry of Education, University and Research (PRIN 2004). The authors also acknowledge the “Consorzio per le Applicazioni di Supercalcolo per Università e Ricerca (CASPUR-Rome)” for the computational facilities.

## REFERENCES

- Zaslhoff, M. *Nature* 2002, 415, 389–395.
- Bulet, P.; Stocklin, R.; Menin, L. *Immunol Rev* 2004, 198, 169–184.
- Boman, H. G. *Annu Rev Immunol* 1995, 13, 61–92.
- Boman, H. G. *J Intern Med* 2003, 254, 197–215.
- Kimbrell, D. A.; Beutler, B. *Nat Rev Genet* 2001, 2, 256–267.
- Hancock, R. E. W. *Lancet Infect Dis* 2001, 1, 156–164.
- Papagianni, M. *Biotechnol Adv* 2003, 21, 465–499.
- McElhaney, R. N.; Prenner, E. J. *Biochim Biophys Acta* 1999, 1462, 1–234.
- Menestrina, G.; Dalla Serra, M.; Lazarovici, P., Eds. *Pore-Forming Peptides and Protein Toxins*; Taylor Francis: London and New York, 2003.
- Rinaldi, A. C.; Mangoni, M. L.; Rufo, A.; Luzi, C.; Barra, D.; Zhao, H.; Kinnunen, P. K. J.; Bozzi, A.; Di Giulio, A.; Simmaco, M. *Biochem J* 2002, 368, 91–100.
- Rinaldi, A. C. *Curr Opin Chem Biol* 2002, 6, 799–804.
- Simmaco, M.; Mignogna, G.; Canofeni, S.; Miele, R.; Mangoni, M. L.; Barra, D. *Eur J Biochem* 1996, 242, 788–792.
- Wade, D.; Silberring, J.; Soliymani, R.; Heikkinen, S.; Kilpeläinen, I.; Lankinen, H.; Kuusela, P. *FEBS Lett* 2000, 479, 6–9.
- Wade, D.; Silveira, A.; Silberring, J.; Kuusela, P.; Lankinen, H. *Protein Pept Lett* 2000, 7, 349–357.
- Wade, D. *Internet J Chem* 5, 2002, <http://www.ijc.com/articles/2002v5/5/>
- Mangoni, M. L.; Rinaldi, A. C.; Di Giulio, A.; Mignogna, G.; Bozzi, A.; Barra, D.; Simmaco, M. *Eur J Biochem* 2000, 267, 1447–1454.
- Rinaldi, A. C.; Di Giulio, A.; Liberi, M.; Gualtieri, G.; Oratore, A.; Schininà, M. E.; Simmaco, M.; Bozzi, A. *J Pept Res* 2001, 58, 213–220.
- Zhao, H.; Rinaldi, A. C.; Di Giulio, A.; Simmaco, M.; Kinnunen, P. K. J. *Biochemistry* 2002, 41, 4425–4436.
- Vignal, E.; Chavanieu, A.; Roch, P.; Chiche, L.; Grassy, G.; Calas, B.; Aumelas, A. *Eur J Biochem* 1998, 253, 221–228.
- Raimondo, D.; Andreotti, G.; Saint, N.; Amodeo, P.; Renzone, G.; Sanseverino, M.; Zocchi, I.; Molle, G.; Motta, A.; Scaloni, A. *Proc Natl Acad Sci USA* 2005, 102, 6309–6314.
- Roccatano, D.; Colombo, G.; Fioroni, M.; Mark, A. E. *Proc Natl Acad Sci USA* 2002, 99, 12179–12184.
- D’Alessandro, M.; Paci, M.; Amadei, A. *Biopolymers* 2004, 74, 448–456.
- Mangoni, M. L.; Saugar, J. M.; Dellisanti, M.; Barra, D.; Simmaco, M.; Rivas, L. *J Biol Chem* 2005, 280, 984–990.
- Mangoni, M. L.; Papo, N.; Barra, D.; Simmaco, M.; Bozzi, A.; Di Giulio, A.; Rinaldi, A. C. *Biochem J* 2004, 380, 859–865.
- Amadei, A.; Chillemi, G.; Ceruso, M. A.; Grottesi, A.; Di Nola, A. *J Chem Phys* 2000, 112, 9–23.
- Evans, D. J.; Morriss, G. P. *Statistical Mechanics of Non-equilibrium Liquids*; Academic Press: London, 1990.
- Darden, T.; York, D.; Pedersen, L. J. *J Chem Phys* 1993, 98, 10089–10092.
- Berendsen, H. J. C.; Postma, J. P. M.; van Gunsteren, W. F.; Hermans, J. In *Intermolecular Forces*; Pullman, B., Ed.; Reidel Publishing Company: Dordrecht, 1981; pp 331–342.

29. van der Spoel, D.; Berendsen, H. J. C.; van Buuren, A. R.; Apol, M. E. F.; Meulenhoff, P. J.; Sijbers, A. L. T. M.; van Drunen, R. GROMACS User Manual. University of Groningen, Groningen, The Netherlands, 1995.
30. Amadei, A.; Linssen, A. B. M.; Berendsen, H. J. C. *Proteins* 1993, 17, 412–425.
31. Di Teodoro, C.; Aschi, M.; Amadei, A.; Roccatano, D.; Malatesta, F.; Ottaviano, L. *ChemPhysChem* 2005, 6, 681–689.
32. Pokorny, A.; Almeida, P. F. F. *Biochemistry* 2004, 43, 8846–8857.
33. Lohner, K.; Blondelle, S. E. *Comb Chem High Throughput Screen* 2005, 8, 241–256.

*Reviewing Editor: Nancy Stellwagen*